Analysis of Hall Current and Rotation in MHD Dusty Fluid Flow over an Impulsively Moving Vertical Plate with Variable Physical Properties

Santana Hazarika
Department of Mathematics Jengraimukh College,
Majuli, Assam,785105

ABSTRACT
The objective of this paper is to examine the unsteady MHD free convection with heat and mass transfer flow of dusty fluid past an impulsive vertical plate in presence of thermal radiation. Both the fluid viscosity and thermal conductivity are assumed to be vary as an inverse linear function of temperature. Effect of viscous dissipation is consideration in the energy equation. Resultant equations are solved numerically by applying the finite difference method. To illustrate the influence of various physical parameters involved in the problem on the velocity, temperature and species concentration of fluid and dust particles are presented graphically. Numerical results of Skin friction, Nusselt number and Sherwood number are also completed and presented in tabular form.

Keywords
Duty fluid, MHD, Finite Difference Method**,** Variable Viscosity and Thermal Conductivity, Vertical plate.

1. INTRODUCTION
The study of rotating fluid is very interesting for its important in various natural phenomena. It has many practical applications in the field of rotating machinery, lubrication, oceanography, computer storage devices, viscometry and crystal growth processes and also many engineering areas. Von Karman [7] *was* first formulated the problem of hydro magnetic flow due to rotating disk. He also used the similarity transform for the governing partial differential equations transformed into the ordinary differential equations. In 1879, the Hall effect was discovered by Hall, a graduate student at John Hopkins University**.** In the presence of a magnetic field, the tendency of electric current to flow across an electric field is called the Hall effect. There is significant effect of Hall current when the magnetic field is strong. Since Hall current induces secondary flow in the fluid so it has great role in determining flow-features of the fluid flow problems. Therefore, the effect of Hall current on MHD fluid flow problems has a very important role. It has important applications in power generator and Hall accelerators as well as flight magneto hydrodynamics.

The phenomenon of dusty fluid flow in which dust particles are distributed in the fluid has considerable practical applications in various fields such as environmental science, petroleum industry, waste water treatment, power plant piping etc. Saffman [12] formulated the theory of dusty fluid in 1962 which the small dust particles are distributed in the fluid. Chaudhary and Jain [1] studied the Hall effect on MHD mixed convection flow of a viscoelastic fluid past an infinite vertical porous plate with mass transfer and radiation. Gireesha et al. [3] studied the effect of Hall current on hydromagnetic boundary layer in rotating dusty fluid. He also assumed that the pressure gradient is varying exponentially. Hossain [6] discussed the effect of Hall current on unsteady hydromagnetic free convection flow near an infinite vertical porous plate. Using finite difference technique, Hazarika [5] studied the Hall effect in a rotating system of transient hydromagnetic couette flow.

The situation of chemical reaction in heat and mass transfer problems have attracted considerable attention due to their wide range applications in many industries such as chemical and hydro metallurgical industries. There are two types of chemical reaction i.e homogeneous and heterogeneous reaction. A homogeneous reaction takes place uniformly in the entire given phase whereas a heterogeneous reaction exists in a restricted region or within the boundary of a phase. The most important example of first-order homogeneous chemical reaction is smog formation. Generally chemical reaction rate depends on the concentration of the species itself. Hayat et al. [4] examined unsteady three-dimensional couple stress fluid flow over a stretching surface with chemical reaction. Prakash et al. [11] presented the combined effects of radiation and chemical reaction on MHD free convection and mass transfer flow of a micropolar fluid with time dependent suction.

The main objective of the present investigation is to extend the work of Seth et al. [13] to investigate the effects of variable viscosity and thermal conductivity on unsteady free convection heat and mass transfer of electrically conducting, viscous, incompressible dusty fluid flow through a porous medium in an impulsively moving infinite vertical porous plate taking into account of Hall current and rotation. The dimensionless governing coupled, non-linear partial differential equations are discritized using Crank- Nicholson formula and the resulting finite difference equations are solved by an iterative scheme based on Gauss Seidel method. The effects of velocity, temperature and concentration for different parameters are studied graphically.

2. MATHEMATICAL FORMULATION OF THE PROBLEM
Consider an unsteady free convective boundary layer heat and mass transfer flow of an incompressible, electrically conducting, viscous, chemically reacting and optically thin radiating dusty fluid past an impulsively moving infinite vertical plate with variable viscosity and thermal conductivity in the presence of porous medium. The plate is taken along x^*-axis in the vertically upward direction and the y^*-axis is taken normal to the plate. A uniform magnetic field is applied perpendicular to the plate. The fluid and plate are rotated with a uniform angular velocity Ω about the y'-axis. Initially, i.e time $t^* \leq 0$, the plate and surrounding fluid are at rest and same temperature T_∞^* and concentration C_∞^*. At time $t^* > 0$, the plate starts moving in the vertical upward direction with uniform velocity u_0 and the wall temperature as well as concentration of the plate are raised to T_w^* and C_w^*. Consider the viscous

dissipation in the energy equation of fluid. The chemical reaction is considered to be homogeneous and of first order in species concentration equations of fluid phase and dust phase. The fluid is considered as a gray, absorbing-emitting radiation. The number density of dust particles is assumed constant throughout the motion. The dust concentration is assumed such that it is not disturbing the continuity and hydro magnetic effects i.e. the continuity equation is satisfied. The temperature is uniform within the particles and the interaction between the particles is negligible. The fluid properties are assumed to be isotropic and constant except fluid viscosity and thermal conductivity.

Since the plate is infinite in the $x^*$and z^*directions, therefore all physical quantities are depend on $y^*$and t^*except pressure. Let $(u^*, v^*, w^*)$and $(u_p{}^*, v_p{}^*, w_p{}^*)$ are the velocity components of fluid and dust particles in the directions of x^*, y^*, z^* respectively. The induced magnetic field generated by fluid motion is negligible in comparison to the applied magnetic field i.e. $\vec{B} = (0, B_0, 0)$. This assumption is valid because magnetic Reynolds number is very small for liquid metals and partially ionized fluids (Cramer and Pai [2]). In this problem no external or applied polarized voltages exist so the effect of polarization of fluid is negligible (Meyer [10]) i.e. $\vec{E} = (0,0,0)$. This corresponds to the case where no energy is added or extracted from the fluid by electrical means.

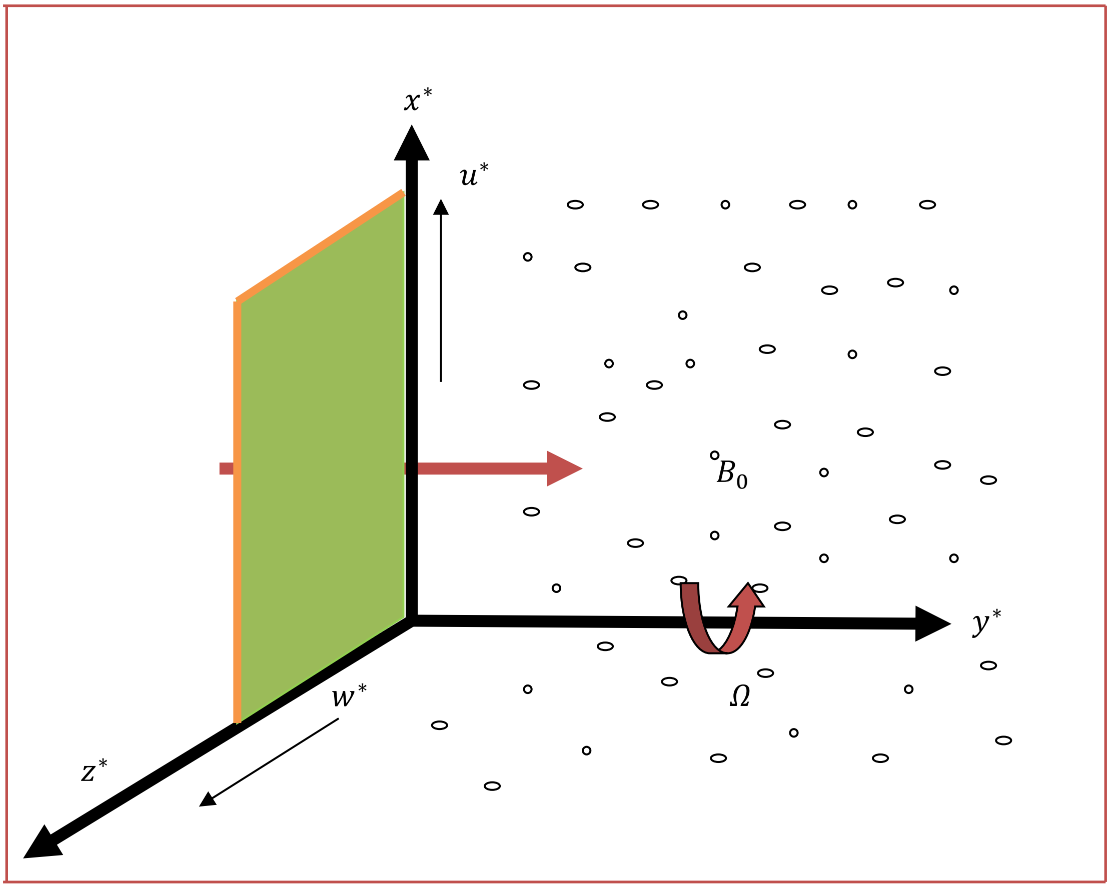

Figure 2.1: Flow configuration

Let $\vec{q} = (u^*, 0,0)$ and $\vec{q}_p = (u_p^*, 0,0)$ denotes the velocities of fluid and dust particles at the point (x^*, y^*, z^*, t^*) in the dusty fluid. Then continuity equations of fluid and dust particles reduce to $\frac{\partial u^*}{\partial x^*} = 0 \Rightarrow u^* = u^*(y^*, t^*)$ and $\frac{\partial u_p{}^*}{\partial x_p{}^*} = 0 \Rightarrow u_p{}^* = u_p{}^*(y^*, t^*)$. Since plate is not porous, so $u^* = 0$ and $u_p^* = 0$.

Under the above assumptions and Boussinesq approximation, the flow governing equations in a rotating frame of reference with Hall current are given by:

Equations of motion for fluid phase:

$$\frac{\partial u^*}{\partial t^*} + 2\Omega w^* = \frac{\partial}{\partial y^*}\left(\nu \frac{\partial u^*}{\partial y^*}\right) + g\beta^*(T^* - T_\infty^*) + g\beta^*(C^* - C_\infty^*) + \frac{KN}{\rho}(u_p^* - u^*) - \frac{\sigma B_0{}^2}{\rho(1+m^2)}(u^* + mw^*) - \frac{\nu}{K_0}u^* \quad ...(2.1)$$

$$\frac{\partial w^*}{\partial t^*} - 2\Omega u^* = \frac{\partial}{\partial y^*}\left(\nu \frac{\partial w^*}{\partial y^*}\right) + \frac{KN}{\rho}(w_p^* - w^*) + \frac{\sigma B_0{}^2}{\rho(1+m^2)}(mu^* - w^*) - \frac{\nu}{K_0}w^* \quad ... (2.2)$$

Equation of energy for fluid phase:

$$\rho c_m \frac{\partial T^*}{\partial t^*} = \frac{\partial}{\partial y^*}\left(k \frac{\partial T^*}{\partial y^*}\right) + \frac{\rho_p c_m}{\tau_T}(T_p^* - T^*) - \frac{\partial q_r}{\partial y^*} + \mu\left[\left(\frac{\partial u^*}{\partial y^*}\right)^2 + \left(\frac{\partial w^*}{\partial y^*}\right)^2\right] \quad ... (2.3)$$

Equation of species concentration for fluid phase:

$$\frac{\partial C^*}{\partial t^*} = \frac{\partial}{\partial y^*}\left(D_m \frac{\partial C^*}{\partial y^*}\right) - K_1^*(C^* - C_\infty^*) \quad ... (2.4)$$

Equations of motion for dust phase:

$$m_p\left(\frac{\partial u^*}{\partial t^*}+2\Omega w_p^*\right)=K\left(u^*-u_p^*\right) \quad ....(2.5)$$

$$m_p\left(\frac{\partial w^*}{\partial t^*}-2\Omega u_p^*\right)=K\left(w^*-w_p^*\right) \quad ..(2.6)$$

Equation of energy for dust phase:

$$\frac{\partial T_p^*}{\partial t^*}=-\frac{1}{\tau_T}\left(T_p^*-T^*\right) \quad ... (2.7)$$

Equation of species concentration for dust phase:

$$\frac{\partial C_p{}^*}{\partial t^*}=\frac{\partial}{\partial y^*}\left(D_p\frac{\partial C_p{}^*}{\partial y^*}\right)-K_2^*\left(C_p^*-C_\propto^*\right) \quad ...(2.8)$$

The initial and boundary conditions for the problem are:

$$\left.\begin{array}{l} t^*\leq 0: u^*=w^*=u_p^*=w_p^*=0,\quad T^*=T_p^*=T_\infty^*, C^*=C_p^*=C_\infty^* \text{ for all } y^* \\ t^*>0:\quad u^*=u_p^*=u_0,\ w^*=w_p^*=0,\ T^*=T_p^*=T_w^*,\ C^*=C_p^*=C_w^* \text{ at } y^*=0 \\ u^*\to 0,\ w^*\to 0,\ u_p^*\to 0, w_p^*\to 0,\ T^*\to T_\infty^*,\ C^*\to C_\infty^*,\ T_p^*\to T_\infty^*, C_p^*\to C_\infty^* \text{ as } y^*\to\infty \end{array}\right\} \quad ... (2.9)$$

For an optically thin gray gas, in the presence of thermal radiation the energy equation reduces to

$$\rho c_m\frac{\partial T*}{\partial t*}=\frac{\partial}{\partial y*}\left(k\frac{\partial T*}{\partial y*}\right)+\frac{\rho_p c_m}{\tau_T}\left(T*_p-T*\right)-16a*\sigma*T*^3{}_\infty\left(T*-T*_\infty\right)+\left[\left(\frac{\partial u*}{\partial y*}\right)^2+\left(\frac{\partial w*}{\partial y*}\right)^2\right]$$

Lai and Kulacki [9] have assumed the fluid viscosity as:

$$\frac{1}{\mu}=\frac{1}{\mu_\infty}\left[1+\zeta(T^*-T_\infty^*)\right]$$

or $\frac{1}{\mu}=b(T^*-T_r)$

where $b=\frac{\zeta}{\mu_\infty}, T_r=T_\infty^*-\frac{1}{\zeta}$ ..(2.10)

In the light of the above Khaund and Hazarika [8] assumed the thermal conductivity as:

$$\frac{1}{k}=\frac{1}{k_\infty}\left[1+\xi(T^*-T_\infty^*)\right]$$

or $\frac{1}{k}=c(T^*-T_k)$

where $c=\frac{\xi}{k_\infty}, T_k=T_\infty^*-\frac{1}{\xi}$ ..(2.11)

where μ_∞ and k_∞ are the coefficient of viscosity and thermal conductivity of the fluid at free stream. b, c, T_r and T_k are constant dependent on physical situations. ζ and ξ are constant based on thermal property of the fluid. In general, $b>0, c>0$ for liquids and $b<0, c<0$ for gases.

In order to normalize the flow model, the following non-dimensional variables are introduced:

$$\left.\begin{array}{l} u=\frac{u^*}{u_0}, w=\frac{w^*}{u_0}, y=\frac{y^*}{u_0 t_0},\quad \theta=\frac{T^*-T_\infty^*}{T_w{}^*-T^*{}_\infty}, \varphi=\frac{C^*-C^*{}_\infty}{C_w{}^*-C_\infty^*}, t=\frac{t^*}{t_0}, \\ t_0=\frac{\nu_\infty}{u_0^2}, u_p=\frac{u_p^*}{u_0}, w_p=\frac{w_p^*}{u_0}, \theta_p=\frac{T_p{}^*-T^*{}_\infty}{T_w{}^*-T_\infty^*},\quad \varphi_p=\frac{C_p{}^*-C^*{}_\infty}{C_w{}^*-C_\infty^*}, \end{array}\right\} \quad ...(2.12)$$

Using (2.10) - (2.12) the equations (2.1) - (2.8) in non-dimensional form

$$\frac{\partial u}{\partial t}+2K_w^2 w=\frac{\theta_r}{(\theta-\theta_r)^2}\frac{\partial\theta}{\partial y}\frac{\partial u}{\partial y}-\frac{\theta_r}{\theta-\theta_r}\frac{\partial^2 u}{\partial y^2}+B\left(u_p-u\right)+Gr\theta+Gm\varphi-\frac{M}{1+m^2}(u+mw)+\frac{1}{K_p}\frac{\theta_r}{(\theta-\theta_r)} \quad ...(2.13)$$

$$\frac{\partial w}{\partial t}-2K_w^2 u=\frac{\theta_r}{(\theta-\theta_r)^2}\frac{\partial\theta}{\partial y}\frac{\partial w}{\partial y}-\frac{\theta_r}{\theta-\theta_r}\frac{\partial^2 w}{\partial y^2}+B\left(w_p-w\right)+\frac{M}{1+m^2}(mu-w)-\frac{1}{K_p}\frac{\theta_r}{(\theta-\theta_r)}w \quad ...(2.14)$$

$$\frac{\partial\theta}{\partial t}=\frac{1}{Pr\left\{\frac{\theta_k}{(\theta-\theta_k)^2}\left(\frac{\partial\theta}{\partial y}\right)^2-\frac{\theta_k}{\theta-\theta_k}\frac{\partial^2\theta}{\partial y^2}-R\theta+\frac{2}{3}B\left(\theta_p-\theta\right)\right\}\frac{\theta_r}{\theta-\theta_r}\left[\left(\frac{\partial u}{\partial y}\right)^2+\left(\frac{\partial w}{\partial y}\right)^2\right]} \quad ..(2.15)$$

$$\frac{\partial\varphi}{\partial t}=\frac{1}{Sc}\left\{\frac{\theta_r}{(\theta-\theta_r)^2}\frac{\partial\theta}{\partial y}\frac{\partial\varphi}{\partial y}-\frac{\theta_r}{\theta-\theta_r}\frac{\partial^2\varphi}{\partial y^2}\right\}-K_1\varphi \quad ..(2.16)$$

$$\frac{\partial u_p}{\partial t}+2K_w w_p=\frac{1}{G}\left(u-u_p\right) \quad ..(2.17)$$

$$\frac{\partial w_p}{\partial t}-2K_w u_p=\frac{1}{G}\left(w-w_p\right) \quad ..(2.18)$$

$$\frac{\partial\theta_p}{\partial t}=L_0\left(\theta-\theta_p\right) \quad ..(2.19)$$

$$\frac{\partial\varphi_p}{\partial t}=\frac{1}{Sc_p}\left\{\frac{\theta_r}{(\theta-\theta_r)^2}\frac{\partial\theta}{\partial y}\frac{\partial\varphi_p}{\partial y}-\frac{\theta_r}{\theta-\theta_r}\frac{\partial^2\varphi_p}{\partial y^2}\right\}-K_2\varphi_p \quad ..(2.20)$$

The transformed initial and boundary conditions are:

$$\left.\begin{array}{l} t\leq 0: u=0, w=0,\ u_p=0, w_p=0, \theta=\theta_p=0, \varphi=\varphi_p=0 \text{ for all } y \\ t>0: u=1, w=0,\ u_p=1, w_p=0, \theta=\theta_p=1, \varphi=\varphi_p=1 \quad \text{at } y=0 \\ u\to 0, w\to 0,\ u_p\to 0, w_p\to 0,\ \theta\to 0,\ \theta_p\to 0,\ \varphi\to 0, \varphi_p\to 0 \text{ as } y\to\infty \end{array}\right\} \quad ..(2.21)$$

The dimensionless parameters are defined as follows:

$$K_p=\frac{K_0 u_0^2}{\nu_\infty^2},\ Sc=\frac{\nu_\infty}{D_m},\ Sc_p=\frac{\nu_\infty}{D_p},\ R=\frac{16a^*\nu^2{}_\infty\sigma^* T_\infty^3}{\rho_\infty u_0{}^2},$$

$$M=\frac{\sigma B_0{}^2\nu_\infty}{\rho_\infty u_0{}^2}Gr=\frac{g^*\beta^*\nu_\infty(T^*{}_w-T_\infty^*)}{u_0^3}, Gm=\frac{g^*\beta^{**}\nu_\infty(C^*{}_w-C_\infty^*)}{u_0^3},$$

$$Ec=\frac{u_0^2}{(T_w*-T_\infty*)c_m}, K_w^2=\frac{\Omega\nu_\infty}{u_0^2}, K_1=\frac{K_1{}^*\nu_\infty}{u_0^2}, B=\frac{KN\nu_\infty}{\rho_\infty u_0{}^2},$$

$$G=\frac{m_p u_0{}^2}{K\nu_\infty}, L_0=\frac{\nu_\infty}{\gamma_T u_0^2}, K_2=\frac{K_2{}^*\nu_\infty}{u_0^2},$$

Coefficient of Skin–friction:

The coefficient of primary skin–friction C_{fx} and secondary skin friction C_{fw} can be defined as

$$C_{fx}=\frac{\tau_x}{\rho_\infty u_0^2}=-\frac{\theta_r}{(1-\theta_r)}\left(\frac{\partial u}{\partial y}\right)_{y=0} \quad ... (2.22)$$

$$C_{fw}=\frac{\tau_w}{\rho_\infty u_0^2}=-\frac{\theta_r}{(1-\theta_r)}\left(\frac{\partial w}{\partial y}\right)_{y=0} \quad ..(2.23)$$

where $\tau_x=\mu\left.\frac{\partial u^*}{\partial y^*}\right]_{y^*=0}$ is the primary shear stress at the plate

and $\tau_w=\mu\left.\frac{\partial w^*}{\partial y^*}\right]_{y^*=0}$ is the secondary shear stress at the plate.

Rate of Heat Transfer:

The Nusselt number is defined by

$$Nu=\frac{\nu_\infty q_w}{k_\infty(T_w^*-T_\infty^*)u_0}=\frac{\theta_k}{(1-\theta_k)}\left(\frac{\partial\theta}{\partial y}\right)_{y=0} \quad .. (2.24)$$

where $q_w=-k\left.\frac{\partial T^*}{\partial y^*}\right]_{y^*=0}$ is the rate of heat transfer of the fluid.

Rate of Mass Transfer:

Therefore, the Sherwood number is given by

$$Sh=\frac{\nu_\infty q_m}{D_m(C_w^*-C_\infty^*)u_0}=\frac{\theta_r}{(1-\theta_r)}\left(\frac{\partial\varphi}{\partial y}\right)_{y=0} \quad .... (2.25)$$

where $q_m=-D_m\left.\frac{\partial C^*}{\partial y^*}\right]_{y^*=0}$ is the rate of mass transfer of fluid.

3. RESULTS AND DISCUSSION

The boundary value problem (2.13) - (2.21) is discritized using Crank- Nicolson finite difference formula and the resulting finite difference equations are solved numerically using an iterative scheme based on Gauss Seidel method. The influences of some physical parameters on both primary and secondary velocities, temperature and species concentration distributions of both fluid and dust particles are expressed graphically. To determine the accuracy of our present study, we have compared the values of primary and secondary skin- friction, Nusselt number and Sherwood number with those values reported by Seth *et al.* [10] for different values of Prandtle number Pr. From Table (3.2.1) and (3.2.2) we have observed that the accuracy of present study is very significant than Seth *et al.* [13].

The following numerical values of various parameters are taken as $\theta_r = 2, \theta_k = 2, Pr = 0.7, Sc = 0.22, Gr = 2, Gm = 2, m = 1.5, B = 0.5, G = 0.5, K_w^2 = 4, K_p = 0.2, Ec = 0.05$ and $t = 2$ unless otherwise stated. The solutions have been found for different values of magnetic parameter (M), viscosity variation parameter (θ_r), thermal conductivity parameter (θ_k), particle concentration parameter (B), Hall parameter (m), Eckert number (Ec), Schmidt number (Sc).

The effect of magnetic field parameter Mon primary and secondary velocities of both fluid and dust particles are presented in figure (3.1.1). It is observed that the primary as well as secondary velocities of both fluid and dust phases decrease on increasing M which implies that magnetic field tends to retard both primary and secondary flow direction of fluid and dust phase. Naturally it means that in the presence of magnetic field, the magnetic force namely Lorentz force is generated which tends to resist the fluid flow and thus reducing its velocity of fluid and dust particles. In figure (3.1.2), the primary and secondary velocities of fluid and dust particles for different values of viscosity variation parameter θ_r are presented. It is clear from this figure that the primary velocity decreases whereas secondary velocity increases of both fluid and dust particles due to increasing values of viscosity variation parameter θ_r. It is noticed from figure (3.1.3) that primary and secondary velocities of both fluid and dust particles decrease due to increasing values of particle concentration parameter$B$. Physically it means that the interaction between the fluid and dust particles molecules increases as the number of particles increases which reduces the velocity of both fluid and dust particles. It is evident from figure (3.1.4) that both primary and secondary velocities of fluid and dust phases increase on increasing Hall parameter m. This is because that as m increases the effective conductive $\left(\sigma/_{1+m^2}\right)$ decreases which reduces the magnetic damping force on the flow direction and this causes velocity is increased.

Figure (3.1.5) displays the effect of viscosity variation parameter θ_r on the temperature profiles of fluid and dust phases. It is found that an increase in viscosity variation parameter leads both the temperatures to increase gradually. Physically it means that increase in viscosity enhances the friction between the layers. When friction increases the generated heat from the friction on the surface is transferred to the flow. This leads to a rise in the surface temperature and the flow is heated. Figure (3.1.6) represents the effect of temperature of both fluid and dust phases for different values of thermal conductivity parameter θ_k. It is clearly observed from this figure that the temperature profiles of both fluid and dust phase decrease with θ_k. Physically it means that as thermal conduction increases the transportation of heat from a hot region to an adjacent colder region increases. Since temperature within the boundary layer is more than the outsides so temperature decreases. The effect of the viscous dissipation parameter i.e. the Eckert number Econ temperature profiles is shown in figure (3.1.7). It is observed that the temperature of fluid phase increases with increase of Eckert number Ec. It is because that the heat energy is stored in the considered fluid due to frictional heating. Moreover, the temperature of particle phase decreases with increasing values of Eckert number Ec.

The effects of viscosity variation parameter θ_r and Schmidt number Sc on concentration profiles of fluid and dust phases are shown in figure (3.1.8) and (3.1.9). From figure (3.1.8) we observed that concentration profiles of fluid phase as well as dust phase decreases with increasing values of θ_r. From figure (3.1.9), it can be concluded that concentration profiles of both phases decrease as Sc increases. Since Schmidt number is inversely proportional to the diffusion coefficient. Therefore, larger values of Schmidt number correspond to a decrease in the concentration field. Figure (3.1.10) presents the concentration profiles for various values of the dimensional chemical reaction parameter K_1. This figure shows that the increasing values of chemical reaction within the boundary layer decreases the concentration profiles. This is consistent with the fact that chemical reaction reduces the solutal boundary layer thickness and increases the mass transfer.

3.1 Figures

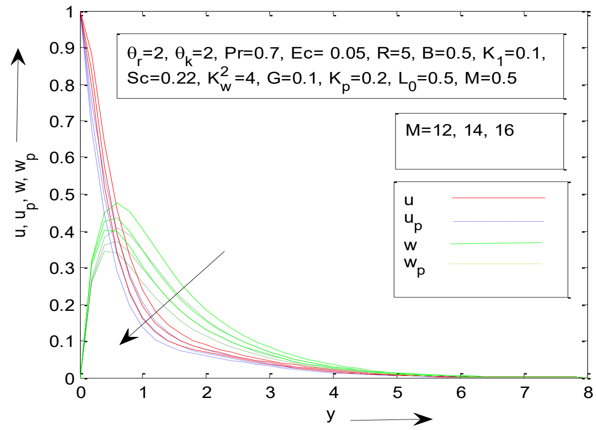

Figure 3.1.1: Primary and secondary velocity profiles of both fluid and dust phases against y for different values of M.

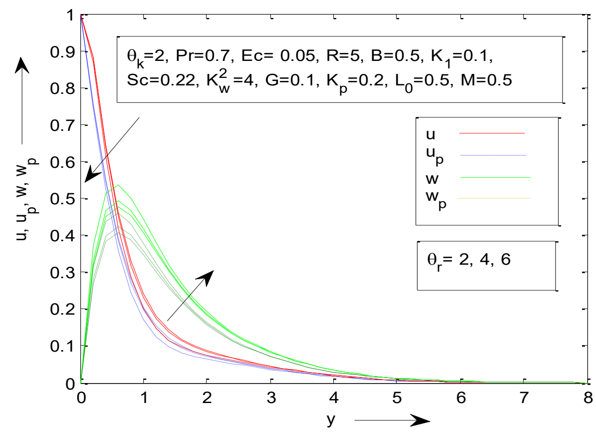

Figure 3.1.2: Primary and secondary velocity profiles of both fluid and dust phases against y for different values of θ_r

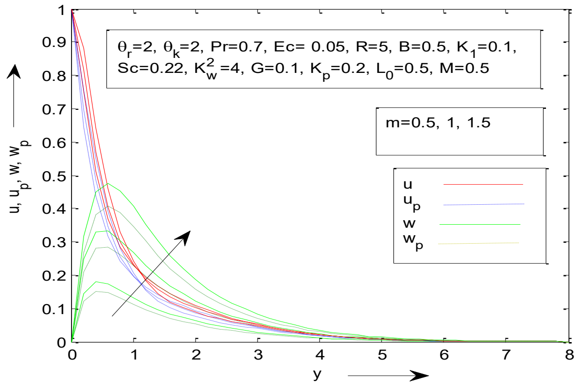

Figure 3.1.3: Primary and secondary velocity profiles of both fluid and dust phases against y for different values of m

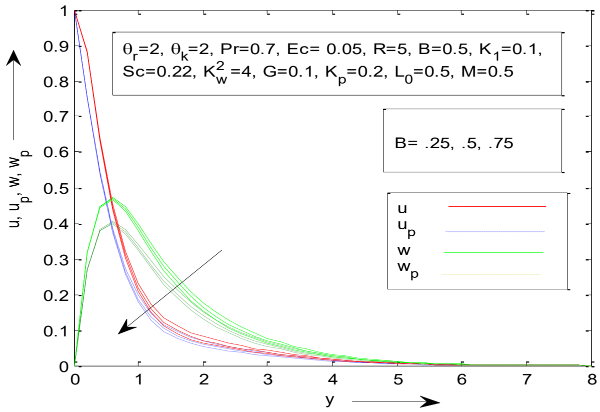

Figure 3.1.4: Primary and secondary velocity profiles of both fluid and dust phases against y for different values of B

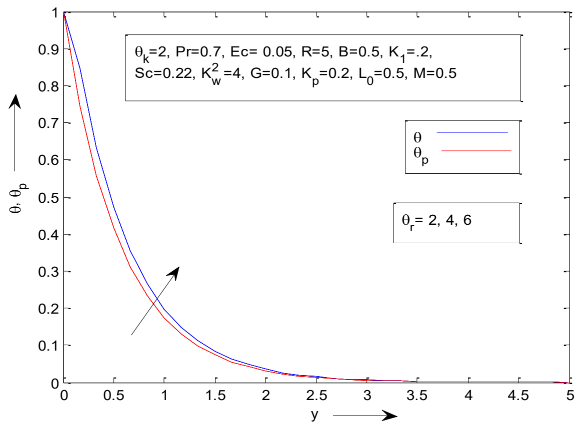

Figure 3.1.5: Temperature profiles of both fluid and dust phases against y for different values of θ_r

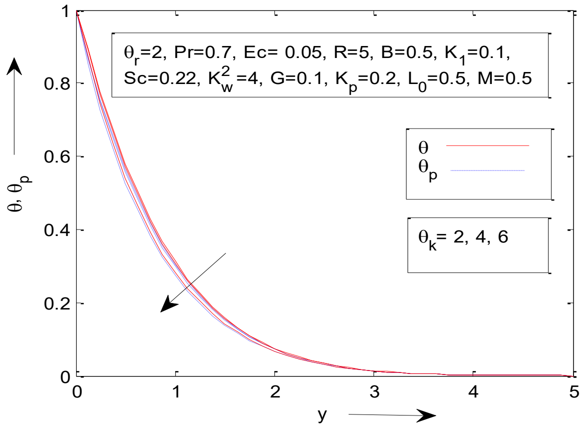

Figure 3.1.6: Temperature profiles of both fluid and dust phases against y for different values of θ_k

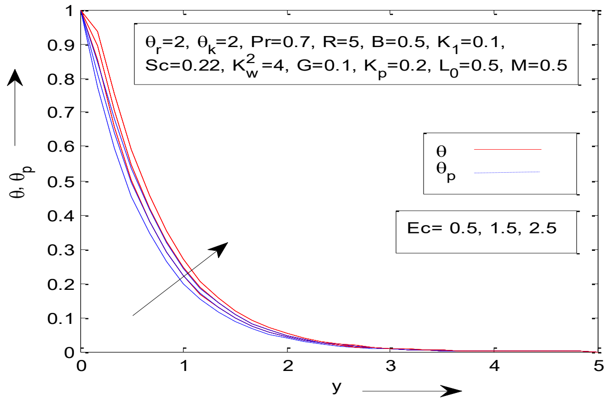

Figure 3.1.7: Temperature profiles of both fluid and dust phases against y for different values of Ec.

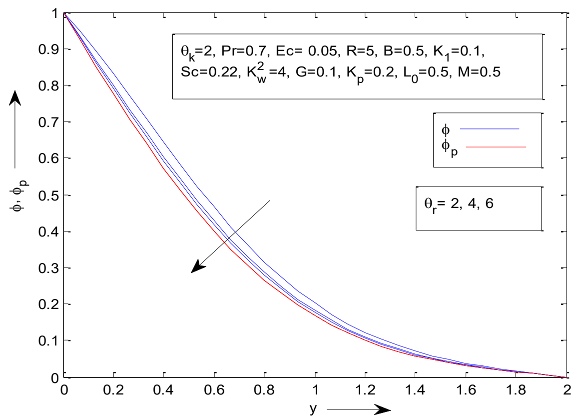

Figure 3.1.8: Concentration profiles of both fluid and dust phases against y for different values of θ_r

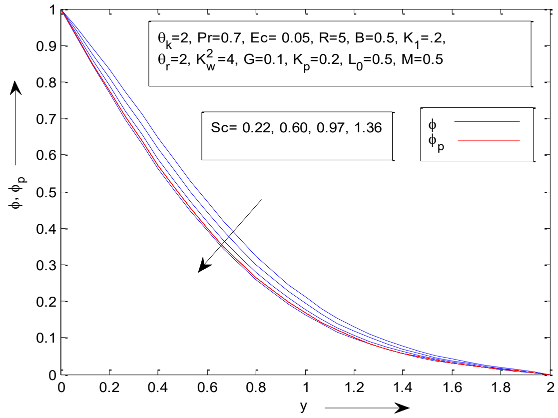

Figure 3.1.9: Concentration profiles of both fluid and dust phases against y for different values of Sc

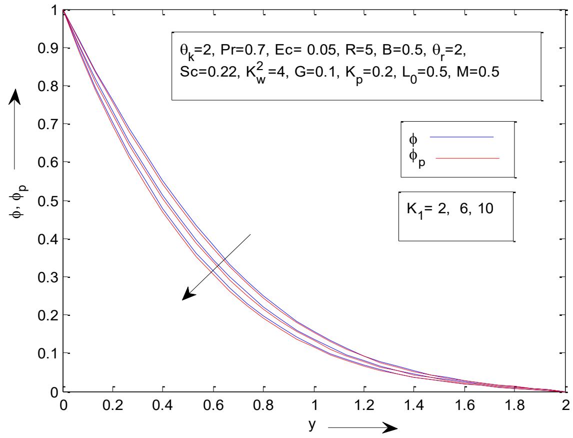

Figure 3.1.10: Concentration profiles of both fluid and dust phases against y for different values of K_1.

3.2 Numerical values of C_{fx}, C_{fw}, Nu and Sh:

Variation of viscosity parameter θ_r, thermal conductivity parameter θ_k as well as magnetic parameter M on primary and secondary skin-friction coefficients, Nusselt number and Sherwood number are estimated numerically in table (3.2.3) - (3.2.5). It is noticed from table (3.2.3) that primary skin-friction coefficient C_{fx}, Nusselt number Nu as well as Sherwood number Sh decrease on increasing θ_r whereas these agencies have reverse effect on secondary skin-friction coefficient C_{fw}. It is noticed from table (3.2.4) that both primary and secondary skin frictions as well as Sherwood number increase on increasing θ_k. This implies that thermal conductivity tends to enhance both primary and secondary skin friction coefficients as well as Sherwood number. Further, the increasing values of θ_k reduces the Nusselt number. It is because that as thermal conductivity increases the viscosity of the fluid decreases which reduces the magnitude of rate of heat transfer. From table (3.2.5), it is observed that the both primary and secondary skin friction coefficients as well as Sherwood number decrease whereas Nusselt number increases with increasing values magnetic parameter M.

Tables for Numerical Values of C_{fx}, C_{fw}, Nu, Sh:

Table 3.2.1:Comparison of the results for C_{fx} and C_{fw}, Nu and Sh for various values of Pr.

Pr	C_{fx}		C_{fw}	
	Present study	Previous study	Present study	Previous study
0.25	1.375226	1.442190	0.053415	1.233845
0.5	1.375411	1.433887	0.053414	1.239221
0.75	1.375607	1.424909	0.053412	1.245071

Table 3.2.2: Comparison of Nu and Sh for various values of Pr

Pr	Nu		Sh	
	Present study	Previous study	Present study	Previous study
0.25	1.538947	1.699226	0.483658	0.502272
0.5	1.470349	1.625596	0.483518	0.502252
0.75	1.398845	1.547574	0.483358	0.502152

Table 3.2.3: Variation of C_{fx},C_{fw}, Nu and Sh for various values of θ_r with $\theta_k = 2, Pr = 0.7, Sc = 0.22, Gr = 2, Gm = 2, m = 1.5, B = 0.5, K_w^2 = 4, G = 0.5, K_p = 0.2, Ec = 0.05$

θ_r	C_{fx}	C_{fw}	Nu	Sh
2	-0.754578	0.046385	1.413389	0.483391
3	-0.922624	0.048407	1.320206	0.236288
4	-1.042297	0.049815	1.301254	0.096807
5	-1.131959	0.050847	1.296065	0.007736
6	-1.201726	0.051631	1.294511	0.005746
7	-1.257644	0.052245	1.294104	0.003593
8	-1.303574	0.052732	1.294124	0.003464
9	-1.342160	0.053120	1.294355	0.002745
10	-1.375567	0.053413	1.294757	0.002648

Table 3.2.4:Variation of C_{fx},C_{fw}, Nu and Sh for various values of $\theta_k$with $\theta_r = 2, Pr = 0.7, Sc = 0.22, Gr = 2, Gm = 2, m = 1.5, B = 0.5, K_w^2 = 4, G = 0.5, K_p = 0.2, Ec = 0.05$

θ_k	C_{fx}	C_{fw}	Nu	Sh
2	-1.375567	0.053413	1.413389	0.483391
3	-1.373937	0.053484	1.315084	0.237272
4	-1.372868	0.053532	1.290476	0.097887
5	-1.372015	0.053570	1.278491	0.007128
6	-1.371271	0.053603	1.268547	0.006167
7	-1.370594	0.053633	1.257521	0.005694
8	-1.369963	0.053660	1.243683	0.005306
9	-1.369365	0.053686	1.225078	0.005194
10	-1.368787	0.053709	1.198410	0.004020

Table 3.2.5: Variation of C_{fx},C_{fw}, Nu and Sh for various values of M with $\theta_r = 2, \theta_k = 2, Pr = 0.7, Sc = 0.22, Gr = 2, Gm = 2, m = 1.5, B = 0.5, K_w^2 = 4, G = 0.5, K_p = 0.2, Ec = 0.05$

M	C_{fx}	C_{fw}	Nu	Sh
2	-1.370200	0.053415	1.259938	0.483684
3	-1.370659	0.053493	1.298790	0.237619
4	-1.371183	0.053541	1.336424	0.098169
5	-1.371791	0.053577	1.373274	0.006938
6	-1.372530	0.053607	1.410716	0.006079
7	-1.373525	0.053634	1.455088	0.005724
8	-1.375191	0.053657	1.552335	0.003478

4. CONCLUSIONS:

This study presents an investigation of the effects of variable viscosity and thermal conductivity on unsteady free convection heat and mass transfer of electrically conducting, viscous, incompressible dusty fluid flow through a porous medium in an impulsively moving infinite vertical plate in the presence of Hall current and rotation. It is found that, the flow field is appreciably affected by Hall current, magnetic parameter, viscosity variation parameter, thermal conductivity parameter and particle concentration parameter. The conclusions of the present study are as follows:

- Hall current accelerates both primary and secondary velocities.
- Magnetic field tends to retard both primary and secondary velocities.
- Viscosity tends to retard primary velocity whereas it has reverse effect on secondary velocity.
- Temperature decreases as thermal conductivity parameter increases.
- Eckert number has tendency to enhance the temperature of fluid phase whereas it has reverse effect on dust phase.
- Concentration decreases as viscosity and Schmidt number increase.

- Thermal conductivity tends to enhance both primary and secondary skin frictions.

5. REFERENCES

[1] Chaudhary R.C., Jain P., Hall effect on MHD mixed convection flow of a viscoelastic fluid past an infinite vertical porous plate with mass transfer and radiation, Theoret. Appl. Mech., Vol.33, No.4, pp. 281-309, 2006.

[2] Cramer K.R., Pai S.I., Magnetofluid dynamics for engineers and applied plysicists, McGraw Hill Book Company, New York, 1973.

[3] Gireesha B. J., Manjunatha S., Lokesh H. J., Bagewadi C. S., Effect of Hall Current on Hydromagnetic Boundary Layer in Rotating Dusty Fluid with Exponential Pressure Gradient**,** IOSR J. of Mathematics, Vol. 10, No. 2, pp. 23-31, 2014.

[4] Hayat T., Awais M., Safdar A., Hend A. A., Unsteady three-dimensional flow of couple stress fluid over a stretching surface with chemical reaction, Nonlinear Analysis Modelling and Control, Vol. 17, pp. 47–59, 2012.

[5] Hazarika G. C., Hall effects in a rotating system of transient hydromagnetic couette flow, Mathematical Forum, Vol. 25, pp. 23-36, 2012-2013.

[6] Hossain M.A., Effect of Hall current on unsteady hydromagnetic free convection flow near an infinite vertical porous plate. J. Phys. Soc. Japan, Vol.55, pp.2183-2190, 1986.

[7] Karman T. V., Uber laminar und turbulent Reibung, Z. Angew. Math. Mech., Vol. 1, No. 4, pp. 233-252, 1921.

[8] Khound P.K., Hazarika G. C., The effect of variable viscosity and thermal conductivity on liquid film on an unsteady stretching surface, Proc. Of 46th Annual tech. Session, Ass. Sc. Soc., pp. 47-56, 2000.

[9] Lai F.C., Kulacki F.A., The effect of variable viscosity on conductive heat transfer along a vertical surface in a saturated porous medium, Int. J. Heat Mass Transfer, Vol. 33, pp. 1028-1031, 1990.

[10] Meyer R.C., Reducing aerodynamic heat transfer rates by magnetohydrodynamic techniques. J. Aero/Space Sci., Vol.25, pp. 561-572, 1958.

[11] Prakash J., Ogulu A., Zhandire E., MHD free convection and mass transfer flow of a micropolar thermally radiating and reacting fluid with time dependent suction, J. Pure and Appl. Phys, Vol. 46, pp. 679-684, 2008.

[12] Saffman P. G., On the stability of laminar flow of a dusty gas, J. Fluid Mech., 12, pp 120-128, 1962.

[13] Seth G. S., Hussain S. M., Sarkar S., Effects of Hall current and rotation on unsteady MHD natural convection flow with heat and mass transfer past an impulsively moving vertical plate in the presence of radiation and chemical reaction, Bulgarian Chem. Comm., Vol. 46, pp. 704 – 718, 2014.

[14] Sharma B. K., Jha A. K., Chaudhary R. C., Hall effect on MHD mixed convective flow of a viscous incompressible fluid past a vertical porous plate immersed in porous with heat source/ sink, Rom. Journn. Phys., Vol. 52, No. 5, pp. 487–503, 2007.